

Modeling Nonlinear Behavior in the Fermilab Main Ring

R. E. Gerig, L. Michelotti, Y. Chao
 Fermi National Accelerator Laboratory*
 P.O. Box 500
 Batavia, IL 60510

Abstract

Recent simulations of the Fermilab Main Ring indicate that the systematic nonlinearities of decapole order and higher lead to chaotic behavior and slow or sudden amplitude growth after many thousand turns. This behavior is seen in the model at emittances very near the measured acceptance of the Main Ring. The simulation and results will be discussed.

1 Introduction

The Fermilab Main Ring has long been a subject of accelerator simulations. Considerable work has been done in attempting to understand the limiting dynamic aperture at the injection energy of 8 GeV. Previous papers have focused on various resonance phenomena and attempts to compensate [1,2]. More recently however, the emphasis has been on the higher order systematic errors in the Main Ring dipoles. These errors manifest themselves in longer term tracking situations where particles may survive for many thousands of turns before departing the aperture.

In this paper only a few models of Main Ring are considered. The discussion that follows addresses the tools which have been employed to understand the dynamic aperture of the model and to understand the nature of the observed emittance growth.

2 The Model

At each stage of the simulation attempts are made to reproduce conditions representing the real Main Ring. This applies to the upper limit of the number of turns which are tracked. In the Main Ring the longest time the beam coasts at 8 GeV is .75 seconds during filling for fixed target physics. This corresponds to 35000 turns. Thus the tracking limit is set to 35000 turns, and particles which survive this long are considered to be 'stable'. The model includes synchrotron oscillations which have the effect of modifying the strength of all kicks, linear and nonlinear, once per turn. In most of the cases presented the peak fractional momentum error was .001. In addition to systematic multipole moments the random components have been included using statistical methods. Previous models have included orbit distortions. In a following section the effect of large orbit distortions are discussed, but most of the work presented in this paper results from a model in which the closed orbit goes through the center of all the elements. The orbit distortions which are used in the Main Ring models are large local three or four bumps which, in the real Main Ring, are used to get around Lambertson transfer magnets. In studying the techniques which were applied to the model the bumps were removed to eliminate the possibility that the observed effects were produced by a single bad place in the ring. They will be reintroduced when the tools for evaluating the model are refined to the point where they can be used in that manner.

Magnetic measurements of dipoles in the Main Ring are the basis for the multipole distribution in the model. Multipoles through 16-pole are included. The numbers have been modified slightly to better reproduce the chromaticity curve as measured in the Main Ring. Figure 1 shows the field in the two styles of Main Ring dipoles. The B1 dipoles have a gap that is 1.4 inches by 5 inches. The B2 dipoles have a gap that is 2.0 inches by 4.0 inches. In the figure the normal field shape is shown with the quadrupole and sextupole subtracted (to illustrate the effect of the uncorrected multipoles). Note that there is no abrupt edge to a good field region. This has the effect of making the dynamic aperture a more difficult thing to determine since there will not be a sharp transition between stable ordered behavior and easily detectable unbounded behavior. It is in this chaotic region that most of the study has been directed. Many of the figures originate from a model in which the decapole was removed. This model was being studied to address the question of the effectiveness of decapole correctors.

*Operated by the Universities Research Association, Inc. for the U. S. Department of Energy

Magnetic Field Shape Of Main Ring Dipoles

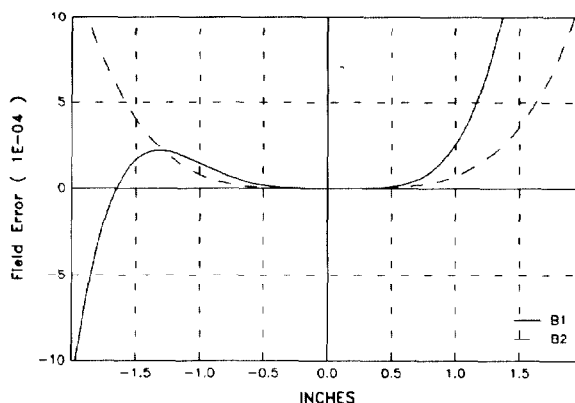


Figure 1: Field Shape in Main Ring Dipoles

3 Long Term Tracking

Figure 2 presents the results of a series of long term tracking runs. A single particle is launched with identical initial amplitudes in both horizontal and vertical normalized phase space. The launch point was maintained along the positive abscissa in both planes so that the initial normalized angles, x/N and y/N are 0.0. The figure illustrates the problem of determining the dynamic aperture by this method in that it requires a large amount of computer time (1000 hours on a Sun 4/110.) Two factors contribute to the large amount of computer time; the number of turns, and the step size of the scan. If fewer turns had been chosen for this model, a different dynamic aperture might have been obtained. The very fine step size of .01 mm was chosen in order to better explore the sensitivity to initial conditions in this region. The small step size is also intended to obviate the need to approach the dynamic aperture from different directions in four dimensional phase space. This would not be the case if the aperture were limited by a low order resonance which would have the effect of contorting phase space into a shape different from a four dimensional sphere. In this model the phase space boundary appears to be spherical although it exhibits microstructure. To verify this, scans are being made from different orientations in four dimensional phase space and so far answers differ by no more than .2 mm. This work is continuing.

In an attempt to determine the dynamic aperture using less computer time than the 'brute force' tracking method, several techniques have been explored. One method uses a Lyapunov exponent algorithm, and another employs the tracking of eigenvalues. Both of these are based on the four by four single turn Jacobian. A third method is based on the behavior of the quantity called smear [3] as the dynamic aperture is approached from the center of the aperture. In addition to simply wishing to speed up the computation is the desire to reveal something about which regions of phase space are potentially dangerous and to be avoided.

4 Jacobian Techniques

Consider the divergence of two infinitesimally close orbits — \mathbf{z} , the "fiducial orbit," and $\mathbf{z} + \epsilon$ — under iteration of a mapping, T . Expanding iterates to first order about the fiducial orbit results in the following sequence of equations.

$$\begin{aligned} \mathbf{z}_n &= T_{n-1}(\mathbf{z}_{n-1}) \\ \mathbf{z}_n + \epsilon_n &= T_{n-1}(\mathbf{z}_{n-1} + \epsilon_{n-1}) \end{aligned}$$

Main Ring Model minus Decapole

Step Size is .01 mm

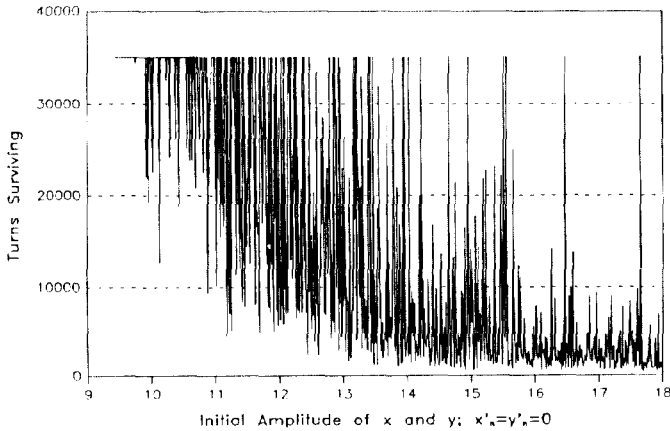


Figure 2: Long Term Tracking Results

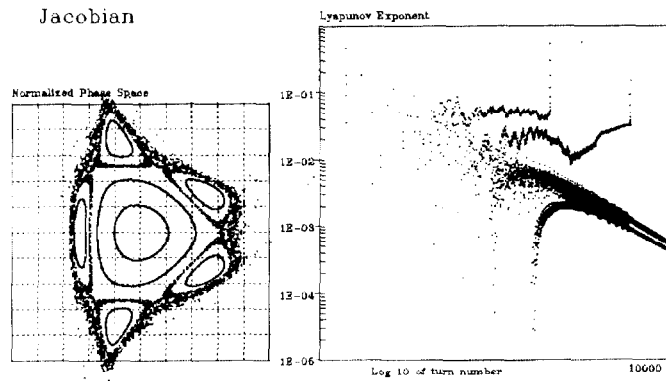


Figure 3: One degree of freedom phase space plot from single sextupole, and corresponding Lyapunov exponent plots

$$\begin{aligned} &= T_{n-1}(\underline{z}_{n-1}) + \epsilon_{n-1} \cdot \underline{DT}_{n-1}(\underline{z}_{n-1}) \\ \therefore \epsilon_n &= \epsilon_{n-1} \cdot \underline{DT}_{n-1}(\underline{z}_{n-1}) \end{aligned}$$

Here, \underline{DT} is the Jacobian of the single-turn map. Notice that the mapping depends on the turn number; this, for example, allows us to include the effect of synchrotron oscillations. If ϵ grows exponentially, then asymptotically we would have

$$|\epsilon_n| \approx |\epsilon_0| \cdot e^{\Gamma n}$$

from which we get the rate,

$$\begin{aligned} \Gamma &\equiv \lim_{n \rightarrow \infty} \frac{1}{n} \ln |\epsilon_n| \\ &= \lim_{n \rightarrow \infty} \frac{1}{n} \sum_{k=1}^n \ln (|\epsilon_k| / |\epsilon_{k-1}|) \end{aligned} \quad (1)$$

For almost all starting values, ϵ_0 , Γ will converge on the largest Lyapunov exponent. If its value is positive, then this indicates exponential divergence of orbits infinitesimally close to the fiducial orbit and, by association, the existence of chaos.

The latter form of Eq.1 indicates how to proceed on a turn-by-turn basis so as to avoid numerical overflow. Since the system is linear, we can "renormalize" before each iteration so that at the beginning of each iterative step, $|\epsilon_{k-1}| \equiv 1$. The single-turn Jacobians are computed automatically by TEVLAT and fed into this algorithm.

The Lyapunov exponent technique has been applied to a single sextupole model as well as to the Main Ring. Figure 3 shows the results for the single sextupole. The traces with a decreasing linear slope correspond to the ordered motion including the orbit in the islands. (The Lyapunov curve from the orbit in the islands is on top of the traces for the two orbits in the central stable region. The island trace was stopped before the end of the plot

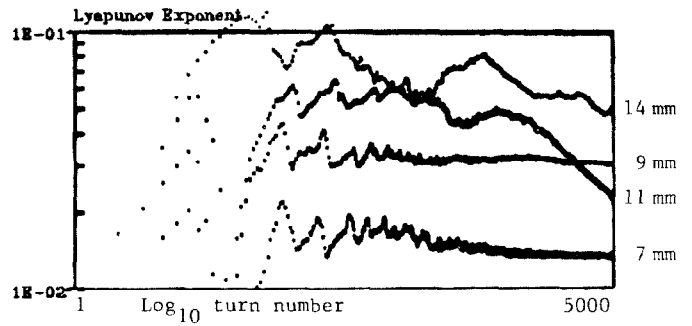


Figure 4: Lyapunov Exponent plots from Main Ring model at initial amplitudes of 14, 11, 9, and 7 mm

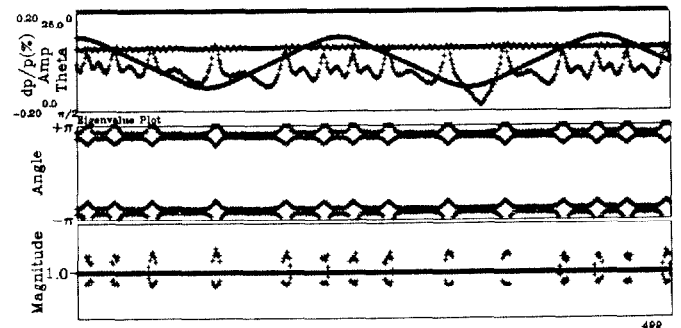


Figure 5: Eigenvalue Analysis

so that the other two could be visible.) The two Lyapunov exponent plots which don't decrease are the chaotic orbits, both of which are lost. Thus the Lyapunov exponent can predict stability in the case of this simple model. The application to the more complicated Main Ring model yields results which are more difficult to interpret. Figure 4 shows the traces for four different initial conditions. The model is the same one used in the tracking shown in Figure 2, so that these results can be compared directly. For large amplitude particles (initial coordinates set to 14 mm) the exponent does not converge and therefore indicates unstable behavior. For small amplitudes defined to be within the dynamic aperture (9 mm and 7 mm) the history of the exponent is converging, although with a very shallow negative slope. For a particle near the dynamic aperture the results are misleading although a 10000 turn calculation at the 11 mm initial conditions indicated that the exponent plot turned up again. Thus it is clear that for this model the exponent must be derived from a calculation involving nearly as many turns as are used in the tracking.

Also of interest are the eigenvalues of the single-turn Jacobians. Because the system is Hamiltonian, these are symplectic matrices, which means their eigenvalues come in reciprocal, complex-conjugate pairs. Eigenvalues off the unit circle indicate a part of the fiducial orbit for which nearby orbits diverge exponentially on a single-turn basis, which suggests resonance-like behavior, perhaps the presence of a nearby separatrix with associated chaotic layer. (Regrettably, remaining on the unit circle does not necessarily mean regular motion: the set of matrices with eigenvalues on the unit circle is not closed under multiplication.)

The results of this analysis are shown in Figure 5. The upper grid displays information directly from the tracking. The flat line is a turn by turn display of the horizontal and vertical amplitudes taken in quadrature. The sinusoidal curve is the momentum of the particle. The erratic curve indicates the extent to which the energy of the particle is in the horizontal or vertical plane. If the coupling were to transfer all of the energy into the horizontal plane then this curve would be at the top of the plot. If the motion is all vertical, then the curve would be at the bottom of the plot as it is at turn 340. The middle grid is used to display the angle of the four eigenvalues, and the lower grid displays the distance of the eigenvalues from the origin. If all four eigenvalues are on the unit circle then this display will simply be a line at the 1.0 level. Two of the eigenvalues can be seen leaving the unit circle indicating instabilities. It can be seen that a.) this occurs more frequently when the particle is at the larger momentum and b.) each time it occurs the

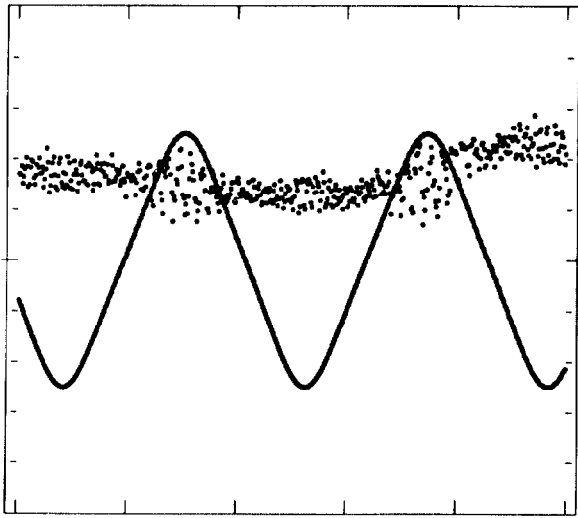


Figure 6: A slice of 500 turns in main ring single particle tracking. The solid line is the dP/P , the points are the quadratic sum of the transverse emittances. The vertical scales are 0.02 per cent per division for dP/P and 0.5 mmmr for the emittance

particle energy is more horizontal than vertical. This is consistent with the Main Ring model which exhibits poorer field quality toward the outside of the aperture.

5 Orbit Analysis

Various approaches have been taken to analyze the behavior of the model in order to understand the cause of the emittance growth. A correlation between the momentum oscillation and transverse emittance growth is observed in the long term tracking. Figure 6 shows the turn by turn plot of dP/P and the quadratically summed transverse emittances from both planes. For large dP/P , or when the particle is carried outward by the RF, a growth in emittance arises. This suggests a stronger nonlinearity toward the outer part of the aperture. Some tracking was done to further pin down the nature of this asymmetry in the horizontal plane.

The distinctly different orbit characteristics between positive and negative dP/P can be caused by asymmetry either in the field content which is seen in Figure 1, or in the closed orbit itself, namely large orbit excursions around transfer devices. To clarify this, a study was carried out to isolate these two effects. The result shows that the asymmetry in field content alone is responsible for the different orbit characteristics for $dP/P < 0$ and $dP/P > 0$.

To determine if an outstanding kick, rather than the distributed nonlinearities, induced the emittance growth when the beam is toward the outside of the aperture, a single turn around the machine was followed with various combinations of initial transverse coordinates and momentum offsets. These values correspond to the extreme dP/P values as shown in Figure 6. Figure 7 shows the vertical one turn orbits with the closed orbit subtracted out. The two lines correspond to momentum offsets of -0.001 and $+0.001$ respectively. Initial transverse coordinates are taken from those corresponding to $dP/P = -0.001$ in a typical run, but a variety of initial coordinates were used to demonstrate that the effect of initial orbit size is not relevant. From Figure 7 it is clear that no outstanding large kick can be held responsible for the amplitude growth when $dP/P = +0.001$, nor can the initial transverse coordinate. The field toward the inside of the aperture actually serves to confine the amplitude of the vertical orbit oscillation. The same effects are not observed in the horizontal motion.

6 Concluding Remarks

The methods discussed in this paper have two objectives. Primarily the goal is to determine the dynamic aperture of a given accelerator model. Tracking provides an answer although many thousands of turns are needed and many initial conditions must be explored. The concept of smear can be used to converge on the dynamic aperture more quickly. Figure 8 shows a plot of smear as a function of amplitude for the same model as shown in Figure 2. The smear, becomes highly sensitive to the initial conditions at 10.1 mm,

the amplitude defined as the dynamic aperture from the tracking shown in Figure 2. The smear was calculated based on tracking for 5000 turns. If 500 turns are used to determine the smear, this approach yields a dynamic aperture at 10.75 mm for this model. Thus it is important to use enough turns in the calculation of the smear, and it appears that the number needed is on the order of 10% of the number needed for straightforward tracking.

Secondly tools are applied to the model in order to gain insight about the features of the model that lead to emittance growth. In particular the eigenvalue technique can provide an early indicator showing that the orbit is visiting regions in phase space that are unstable on a single or few turn basis.

VERTICAL ORBITS

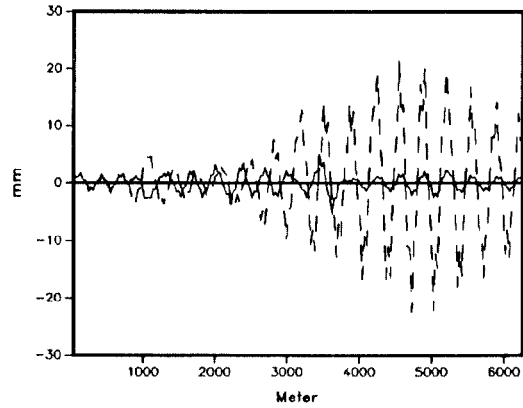


Figure 7: Single turn with closed orbit subtracted. Solid line: $dP/P = -0.001$, Dotted line: $dP/P = +0.001$.

Main Ring Model minus decapole

Step Size is .1 mm

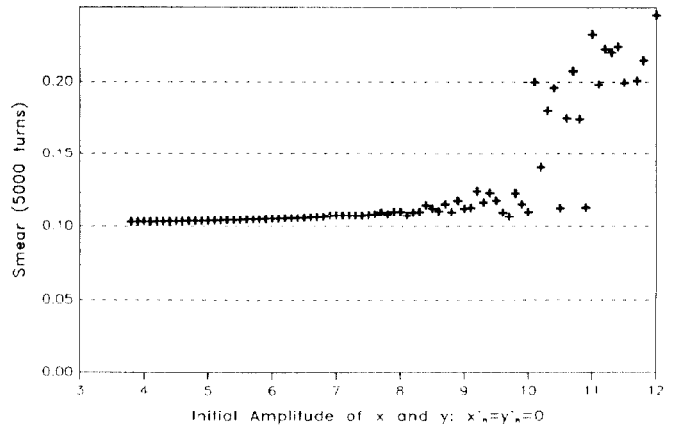


Figure 8: Smear as a function of Amplitude

References

- [1] R. Gerig, et. al., *Proceedings of the 1987 IEEE Particle Accelerator Conference*, 1987, pp. 1123
- [2] R. Gerig, et. al., "Improvements to the Fermilab Main Ring," presented at the European Particle Accelerator Conference, Rome, Italy, June 7-11, 1988.
- [3] A. Chao, et. al., "Experimental Investigation of Nonlinear Dynamics in the Fermilab Tevatron," *Physical Review Letters*, vol. 61, num. 24, pp. 2754, 12 Dec. 1988.